

LARGE EDDY SIMULATION (LES) OF FLOW AND DISPERSION AROUND AN ISOLATED CUBIC BUILDING

Rafael Sartim, rsartim@gmail.com

Neyval Costa Reis Jr., neyval@gmail.com

Universidade Federal do Espírito Santo, Centro Tecnológico, Departamento de Engenharia Ambiental, Av. Fernando Ferrari, 514, 29060-970, Vitória, ES, Brasil

Jane Méri Santos, janemeri@npd.ufes.br

Universidade Federal do Espírito Santo, Centro Tecnológico, Departamento de Engenharia Ambiental, Av. Fernando Ferrari, 514, 29060-970, Vitória, ES, Brasil

Marcos Vinicius Carrijo Fraga, marcoscfsantos@hotmail.com

Universidade Federal do Espírito Santo, Centro Tecnológico, Departamento de Engenharia Ambiental, Av. Fernando Ferrari, 514, 29060-970, Vitória, ES, Brasil

Sandra Paule Beghi, Sandrabeg@yahoo.fr

Universidade Federal do Espírito Santo, Centro Tecnológico, Departamento de Engenharia Ambiental, Av. Fernando Ferrari, 514, 29060-970, Vitória, ES, Brasil

Abstract. *The presence of a building profoundly alters the atmospheric turbulent flow structure. The building not only disturbs the mean wind field, but also increases the turbulence nearby, by generating a large amount of shear stress in the flow. These effects considerably modify the pattern of pollutant dispersion. The complexity of the fluid flow pattern represents a considerable challenge for turbulence models, mainly due to the characteristic boundary layer separations on the sides of the building and the large recirculation regions at the wake of the building. There are several reported studies available in the literature using different turbulence model, with varying levels of accuracy and complexity, ranging from standard k-ε model to Differential Stress Models (DSM). More recent studies point out that Large Eddy Simulation (LES) is the most promising model for this class of problems. The aim of this work is to investigate the flow and dispersion of contaminants in the vicinity of a complex shaped building using LES to model the turbulence effects. The study is based on numerical simulation of the governing equations and was carried out with ANSYS-CFX software. Simulations based on different building orientations relative to the wind direction were studied. A critical aspect of the problem is the time-dependent turbulent inflow conditions. In the present work, turbulent inflow conditions were determined, and the results using rough and smooth surfaces were compared. In order to analyze the accuracy of the proposed model, previous experimental studies were used to validate the results. The comparisons indicate that the model presents reasonable agreement with the experimental study data when a rough surface is used to generate the inflow.*

Keywords: *atmospheric dispersion, large eddy simulation, turbulence modeling*

1. INTRODUCTION

The air pollution involves changes in composition and properties of the air; it is mainly due to the high growth of cities and industrial development. The air quality has an impact on wildlife and human health.

In order to prevent and reduce the air pollution, it is necessary to check the air quality to assess the population exposure degree to pollutants. The air pollution monitoring at the emission source and in the environment are a mean to control. However, high cost analyses can difficult the monitoring or in cases of environmental impact assessment of a future pollution source, mathematical models are useful tools to calculate the atmospheric dispersion of pollutants.

The presence of a building profoundly alters the atmospheric turbulent flow structure. The building do not only disturb the mean wind field, but also increases the turbulence nearby by generating a large amount of shear stress in the flow. These effects considerably modify the pattern of pollutant dispersion The complexity of the fluid flow pattern represents a considerable challenge for turbulence models, particularly due to the characteristic boundary layer separations on the sides of the building and the large recirculation regions at the wake of the building (Mavroids et al. 2007). It represents a challenge for turbulence modeling and its effects on dispersion of pollutants (Santos, 2000).

Flow predictions around a single building based on various turbulence models, such as k-ε models, Differential Stress Models (DSM) and Large Eddy Simulation (LES) were investigated by numerous authors Murakami (1993), Murakami (1997), Rodi (1997), Jiang e Chen (2001), Iaccarino et. al (2003), Senthoooran et. al (2004,), Yakhot et. al (2006). Overall, significantly better predictions were obtained by the LES method, which reasonably simulated the complex features of the flow, even quantitatively. Various works appeared in the literature using the LES for the simulation of flow around obstacles, such as Lübcke et al.(2001).

Currently, the major challenge of the numerical simulation of pollutant dispersion around obstacles is to prescribe time-dependent turbulent inflow conditions at the upstream boundary. The velocity profiles of the inflow should accurately represent a typical wind environment, because it determines the levels of turbulence intensity and therefore the dispersion of pollutants in the environment. Several authors studied various methods to generate these velocity profiles, Lund et al. (1998), Nozawa and Tamura (2002) and Castro (2009). Most of these authors performed a separate "precursor domain" simulation of the approach flow in order to generate the inflow data to be use in the main domain where the building is located. Those techniques are based on the Lund's method that basically consists on estimating the velocity at the inlet plane based on computed velocities downstream and applying outflow boundary conditions at the exit boundary (see Figure 01).

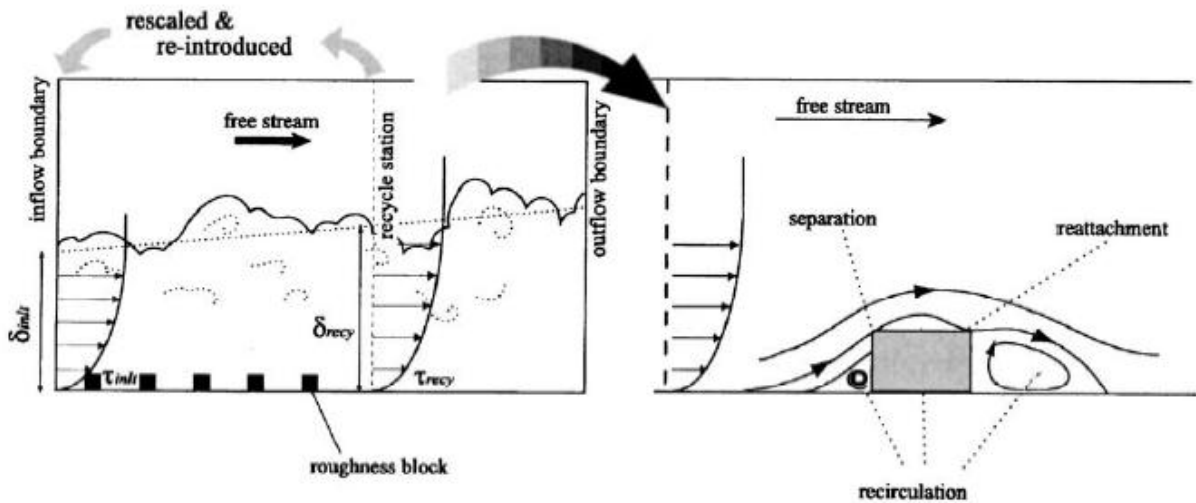


Figure 01 – Schematic presentation of computation. Left: generation of turbulent inflow data; right: simulation of wind flow around a low-rise building. Nozawa and Tamura (2002).

In the present work, the flow and dispersion of contaminants in the vicinity of a complex shaped building were investigated by using LES. Wind flows around a building were simulated in three different situations. Firstly, the west wind direction impinged on the larger face of the building. Secondly, the south wind direction impinged the shorter face of the building. Thirdly the method used consists of single domain containing high-density roughness elements located close to the inlet with a west wind direction impinging on the larger face of the building. In order to assess the accuracy of the results, they were compared with field experiments results obtained by Santos et al (2005).

2. MATHEMATICAL MODELLING

2.1. Fundamental Equations

In this simulation, the fluid flow and contaminant dispersion processes are governed by the conservation equations of mass, momentum and mass of the chemical species (dispersion). These equations are presented below, in their complete form for Newtonian fluids.

Continuity equation

$$\frac{\partial \rho}{\partial t} + \frac{\partial (\rho U_i)}{\partial x_i} = 0 \quad (1)$$

Momentum equation

$$\frac{\partial \rho U_i}{\partial t} + \frac{\partial (\rho U_i U_j)}{\partial x_j} = \frac{\partial \tau_{ij}}{\partial x_j} - \rho g \delta_{3i} \quad (2)$$

where

$$\tau_{ij} = 2\mu S_{ij} - \left(p + \frac{2}{3}\mu \frac{\partial U_k}{\partial x_k} \right) \delta_{ij} \quad (3)$$

and

$$S_{ij} = \frac{1}{2} \left(\frac{\partial U_i}{\partial x_j} + \frac{\partial U_j}{\partial x_i} \right) \quad (4)$$

Concentration equation

$$\frac{\partial(\rho\omega)}{\partial t} + \frac{\partial(U_i\omega)}{\partial x_i} = \frac{\partial}{\partial x_i} \left(\rho D_m \frac{\partial \omega}{\partial x_i} \right) + M \quad (5)$$

U_i , p , t and ω are the component of velocity in the i -direction, thermodynamic pressure, time and mass fraction of a contaminant, respectively. ρ , μ are the density and viscosity, respectively. D_m is the molecular diffusivity of the contaminant and M is the sources of mass of contaminant.

2.2. Turbulence modeling

The performance of CFD prediction of flow around a bluff body based on various turbulence models were investigated by several authors. However, computation using Large Eddy Simulation (LES) provides better estimation accuracy than other turbulence models (Murakami, 1993; Murakami and Mochida, 1996; Cheng et al., 2003). The standard Smagorinsky subgrid model was applied in this simulation.

The Smagorinsky model can be thought of as combining the Reynolds averaging assumptions with a mixing-length based eddy viscosity model for the Reynolds SGS tensor. It is, thereby, assumed that the SGS stresses are proportional to the modulus of the strain rate tensor.

$$\tau_{ij}^s - \frac{1}{3} \tau_{kk}^s \delta_{ij} = \mu_t \left(\frac{\partial \bar{U}_i}{\partial x_j} + \frac{\partial \bar{U}_j}{\partial x_i} \right) = 2\mu_t \bar{S}_{ij} \quad (6)$$

μ_t is the SGS viscosity and \bar{S}_{ij} is the strain rate tensor of the filtered large-scale flow. Based on dimensional analysis, the SGS viscosity can be expressed as:

$$\mu_t = C_s^2 \rho \Delta^2 |\bar{S}| \quad (7)$$

For the Smagorinsky model, C_s is the Smagorinsky constant, which value depends on the type of flow and mesh resolution, Δ is the length scale of the unresolved motion and $|\bar{S}| = (\bar{S}_{ij} \bar{S}_{ij})^{1/2}$. The value used for the Smagorinsky constant is $C_s = 0,15$.

2.3. Boundary Conditions

There are six domain boundaries where the appropriate boundary conditions must be described.

At the two laterals boundaries and the top of the domain, the wall boundary is set to be a Free-slip one, where the shear stress at the wall is zero, and the velocity near wall is not retarded by wall friction effects.

At the outlet boundary, the derivatives of all properties in the main direction are set to zero.

At the ground surface and the building walls, the non-slip condition is assumed. The gaseous contaminant mass flux at the ground surface is zero.

At the inlet boundary, U_2 and U_3 (Y and Z directions respectively) are considered to be equal to zero and the wind velocity profile is provided by the mean velocity values at the entrance of the wind tunnel experiments performed by Sada and Sato (2002).

2.4. Non-dimensional Parameters

It is convenient to present the main parameters in terms of dimensionless variables. This facilitates the analysis and comparison of results for a wide range of physical situations. Thus, the dimensionless forms are:

$$X_i = \frac{x_i}{H_b} \quad U_i = \frac{\bar{U}_i}{U_{Hb}} \quad t^* = \frac{tU_b}{H_b} \quad \omega^* = \frac{\rho\omega U_b H_b^2}{Q} \quad (8)$$

where X_i and U_i are the dimensionless coordinates and velocity components in each direction i . t^* and ω^* are respectively, time and concentration in dimensionless form. Q is the volumetric flow of the pollutant in m^3 / s , and it was considered that the density of the mixture (air + clean) is equal to air density (ρ). U_b is the speed of wind in the main flow direction at the height of the building.

3. NUMERICAL METHOD

The partial differential equations were solved using the finite volume method, for this calculations a CFD code ANSYS CFX-11 were used. The equations were discretized using the central difference advection scheme and the Second Order Backward Euler for the transient scheme. The system of linear algebraic equations produced by the discretization of the equations was solved using a multigrid technique. The ANSYS CFX 11 uses a particular implementation of Algebraic Multigrid called Additive Correction.

As stated earlier, there are three different simulations. The first configuration is shown in Figure 02, in this simulation the direction of the longer wall of the building is normal to the mean direction of velocity. This represents the west wind direction impinging on the larger face of the building. The mean velocity values at the entrance of the calculations domain are the same as those obtained in field experiments performed by Santos (2005) where U_b is wind speed at the building height and its value is 4,61 m/s. The position of the building with height of 3,4 m ($=H_b$) is located $24H_b$ downstream of the entrance of the calculation domain which has the horizontal plane covering $45 H_b$ axially, $40 H_b$ laterally and $10 H_b$ vertically.

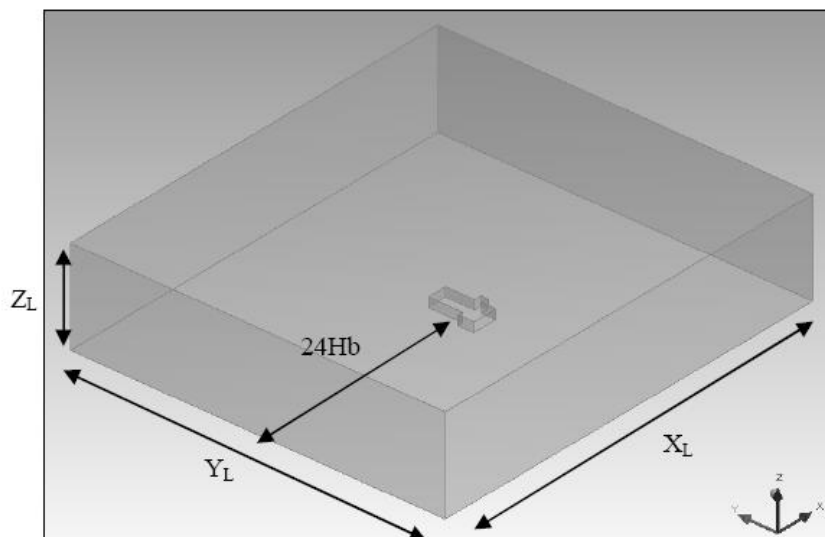


Figure 02 - Schematic representation of the computational domain with the wind impinging on the larger wall of the building.

The second configuration represents the south wind direction (see Figure 03). The wind impinges on the shorter wall of the building. The calculation domain is $45 H_b$, $30 H_b$ and $10 H_b$ for X, Y, Z, the downwind, horizontal and vertical, directions, respectively and the buildings distance from the entrance is $22 H_b$. The U_b value is 6,15 m/s.

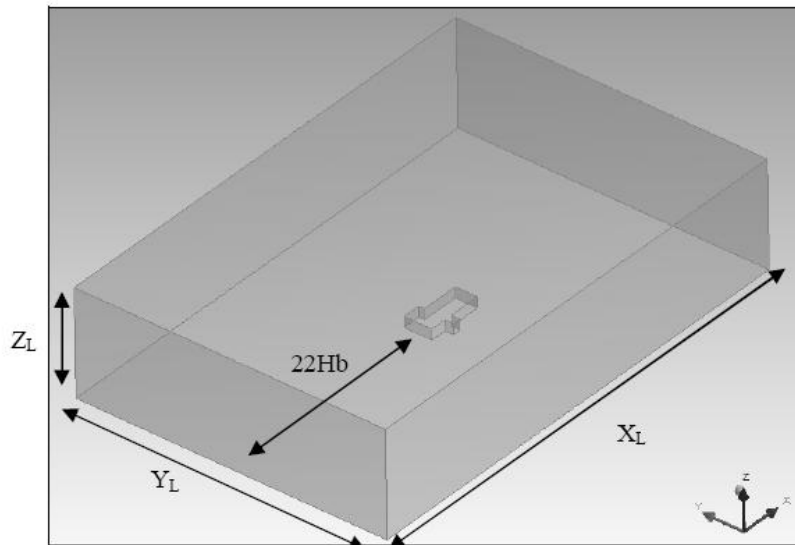


Figure 03 - Schematic representation of the computational domain with the wind impinging on the shorter wall of the building.

The last configuration is similar to the first one where the wind impinges on the shorter wall of the building, however, the inflow reaches the building differently. In this simulation, an approach based on the technique proposed by Nozawa and Tamura (2002) was used. This approach simulates a spatially evolving boundary layer which develops over relatively high-density roughness. In the present work, the simulation is performed in a single domain containing the rough wall elements and the building as shown in Figure 04. The calculation domain is $45 H_b$, $30 H_b$ and $10 H_b$ for X, Y, Z. The rough wall consists of six rows of six cubic elements each with a height of H_b .

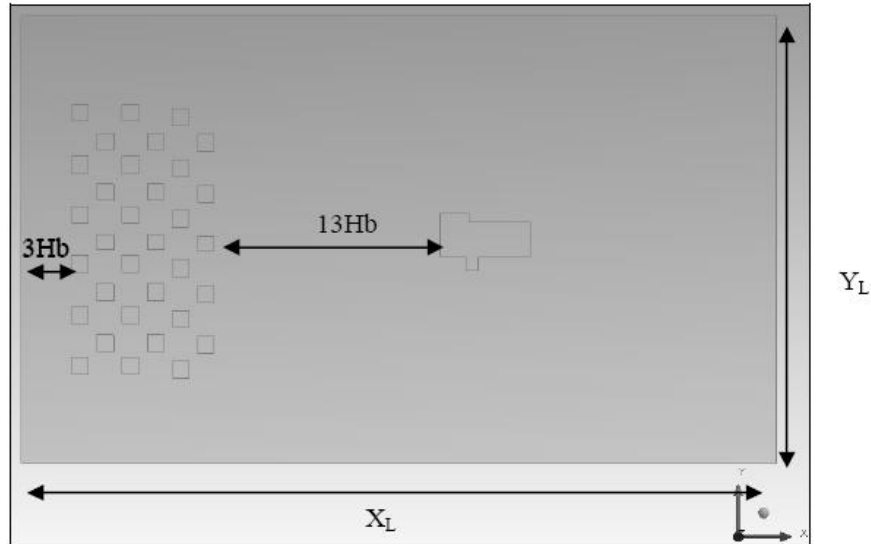


Figure 04 - Schematic representation of the computational domain with the wind impinging on the shorter wall of the building and the high-density roughness elements located close to the inlet.

To assess the mesh sensitivity, in order to investigate the independence of the results according to the mesh resolution, unstructured grids with the amount of elements varying from 100.000 to 500.000 nodes were used. The thinnest mesh was chosen to perform the final results (see Figure 5).

To provide the level of computing required, this numerical simulation was carried out in parallel processing using a PC cluster with 32 processing cores to perform the simulations.

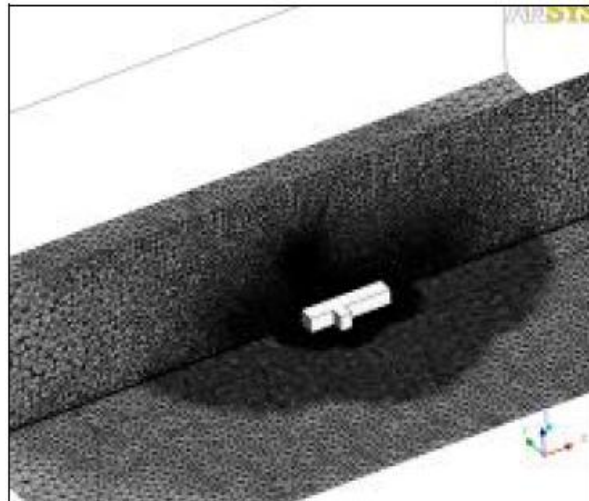


Figure 05 - Mesh used to perform final results. view of the central and ground plane.

The experimental data used for comparison of the simulation results were obtained through the experimental work of Santos et al (2005). The field experiments were conducted at Dugway Proving Ground, 85 miles south west of Salt Lake City in Utah, USA. The experiment involved placing a source of propylene gas at a fixed distance from the building and using gas detectors (photo ionization detectors - PID) to measure concentration close to the walls and on the roof of the building. Figure 06 represents a view of the building used in the trials and shows a schematic representation of the site, indicating the location of the gas source and the PIDs. The xyz co-ordinate system is specified here, respectively, as the along wind direction, the lateral and vertical directions. The source was located up wind at distance of about 3.5 building heights ($x=3,5 H_b$) from the face of the building, at a height of $0,5 H_b$. The source released propylene gas through an open-ended pipe of about 1 cm diameter with a flow rate of 501 l/min.

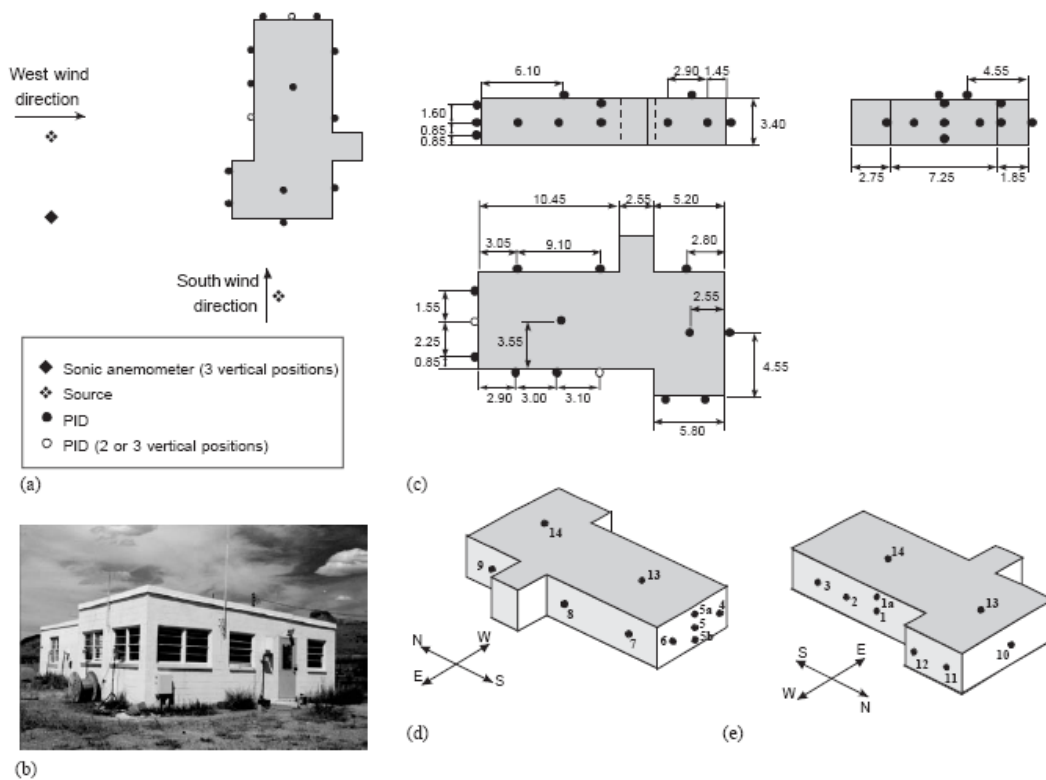


Figure 06 – (a) Schematic representation of the site, (b) photograph of the building used in the experiments at Dugway Proving Ground, (c) top, west and south views (clockwise) of the building and detector location on the building surface, (d) a schematic representation of the detector location and numbering on the building surfaces - perspective view looking from SE – and (e) perspective view looking from NW. (Santos *et al*, 2005).

4. RESULTS

Figure 7 presents the normalised mean concentration on the building walls. Figure 7a and 7b present the concentration distribution on the building walls for the west wind direction (Exp. 3 and 4, numerical simulation, neutral stability) and for the south wind direction (Exp. 1 and 2, numerical simulation, neutral stability), respectively. The corresponding results for, neutral stability, the wind impinging on the shorter wall of the building is presented in Fig. 7c. In this graphic, the numerical solution represents the flow around the building by the influence of turbulence structures created by the high-density roughness placed close to the inlet of the domains as showed in Figure 4.

In the west wind direction condition, Figure 7a, the side walls concentrations were underestimated, while the posterior wall and the central monitor wall previous concentration values were overestimated. The same pattern can be seen, with the south wind direction condition, Figure 7b, except the left lateral wall which overestimated the concentration. This may happen due the low turbulence intensity that impinges on the building, since the velocity profile of the inlet is an average profile used without fluctuations. Therefore, the absence of turbulent motions causes less dispersion of the plume which generates a high concentration in the central detector of the windward wall and low concentrations at the lateral walls. When the wind impinges on the shorter wall of the building with the high-density roughness placed close to the inlet of the domains, a higher dispersion of the plume is observed, Figure 7c. This is due to the presence of high-density roughness elements which increases the turbulence intensity levels. The concentration in the central detector at the windward wall was in good agreement to that obtained in experiment field; this fact also improved the values of the leeward wall and side walls. In

Figure 8c shows that the presence of the high-density roughness elements generated coherent turbulence structures. The intensity fluctuation of the concentration as well as the values calculated corresponds to the experimental data which does not occur in the cases presented in Figures 8a and 8b.

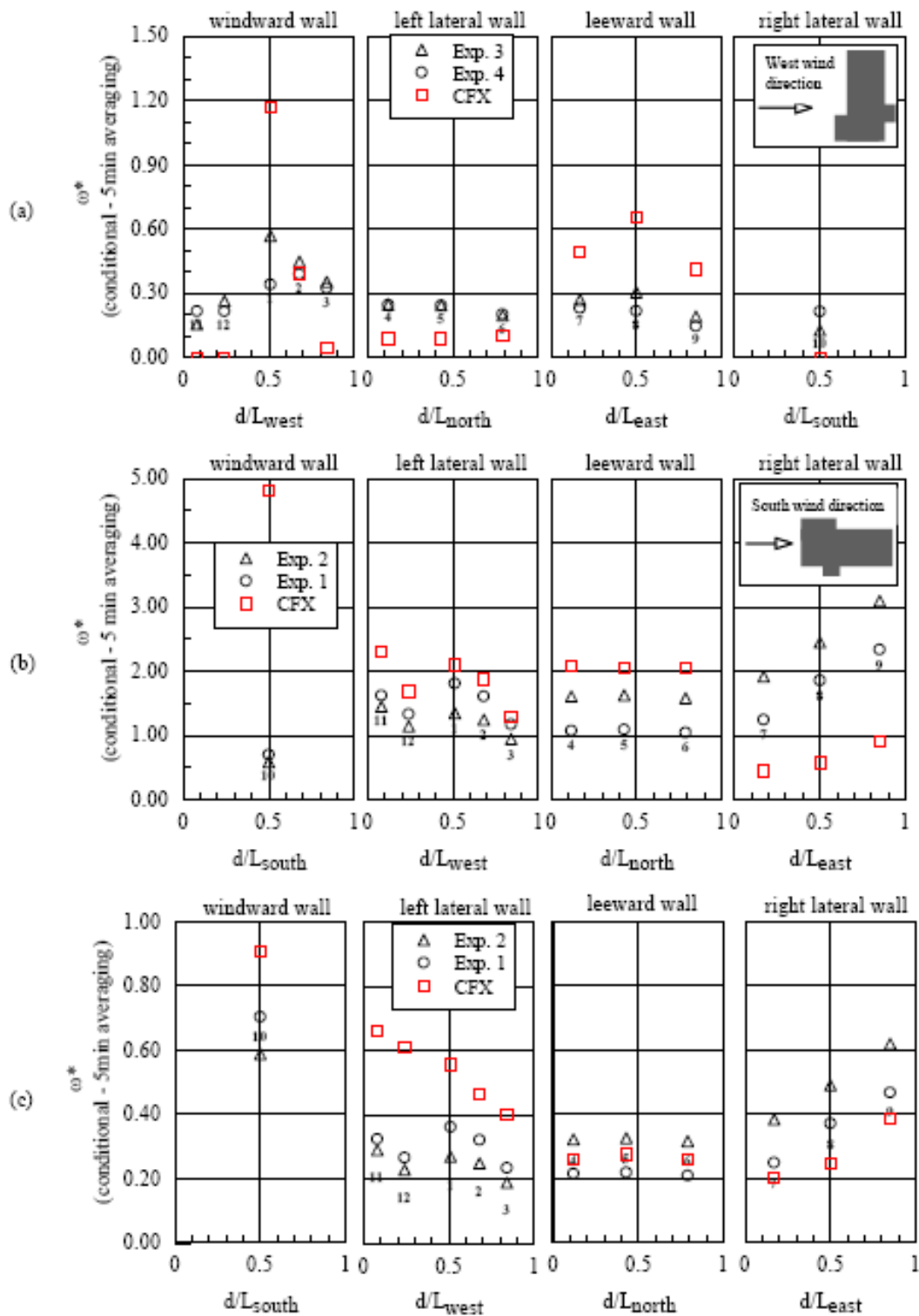


Figure 07 - Conditional normalised mean concentration in (a) neutral conditions for source located upwind of the centre of the long face of the building (Δ Exp. 3 and \circ Exp. 4 Santos et al.(2005), \square simulation), (b) neutral conditions for source located upwind of the centre of the short face of the building (Δ Exp. 2 and \circ Exp. 1 Santos et al.(2005), \square simulation), (c) neutral conditions for source located upwind of the centre of the short face of the building (Δ Exp. 2 and \circ Exp. 1 Santos et al. (2005), \square simulation with high-density roughness).

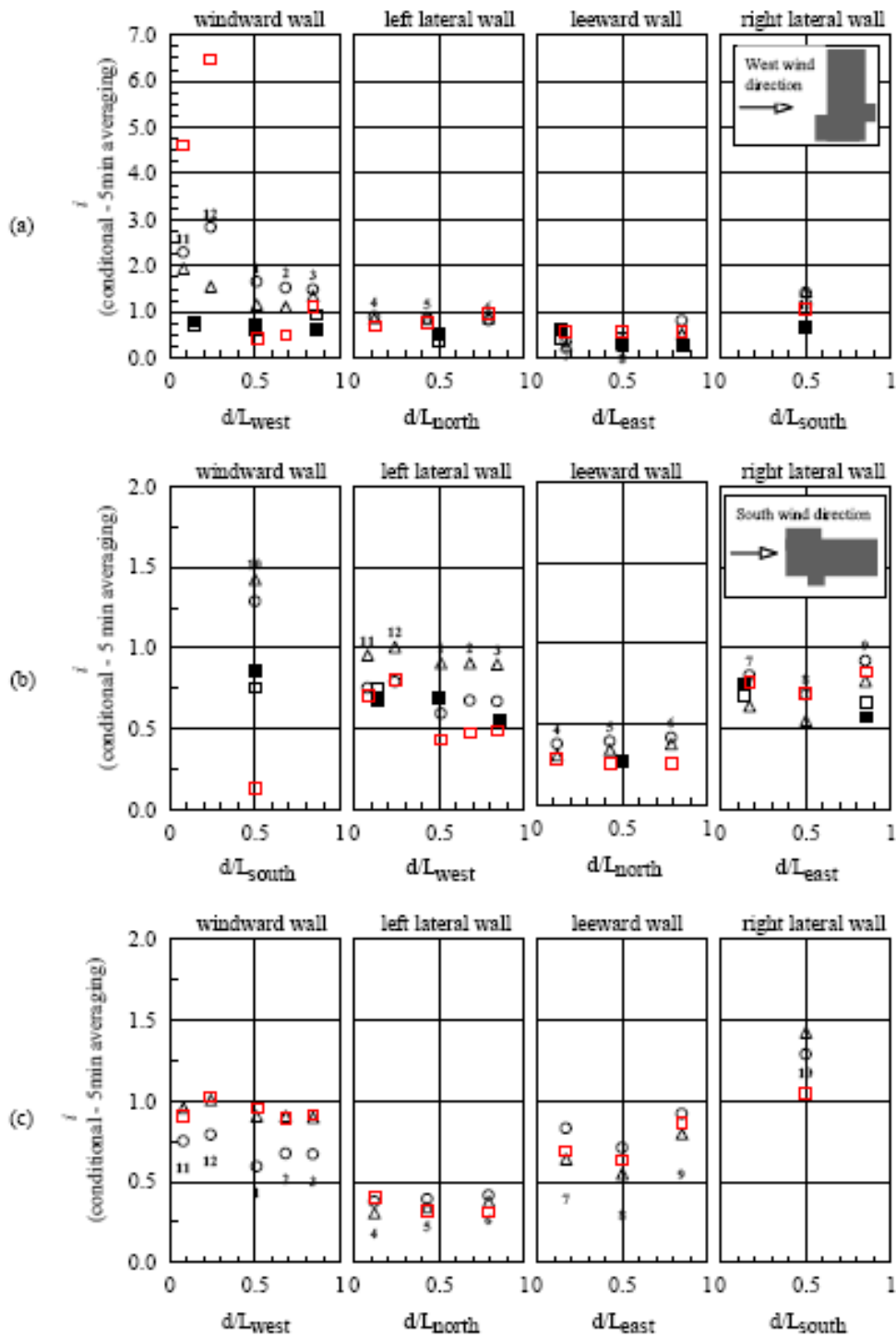


Figure 08 – Conditional concentration fluctuation intensity in (a) neutral conditions for source located upwind of the centre of the long face of the building (Δ Exp. 3 and O Exp. 4 Santos et al. (2005), \square simulation), (b) neutral conditions for source located upwind of the centre of the short face of the building (Δ Exp. 2 and O Exp. 1 Santos et al. (2005), \square simulation), (c) neutral conditions for source located upwind of the centre of the long face of the building (Δ Exp. 2 and O Exp. 1 Santos et al. (2005), \square simulation with high-density roughness)

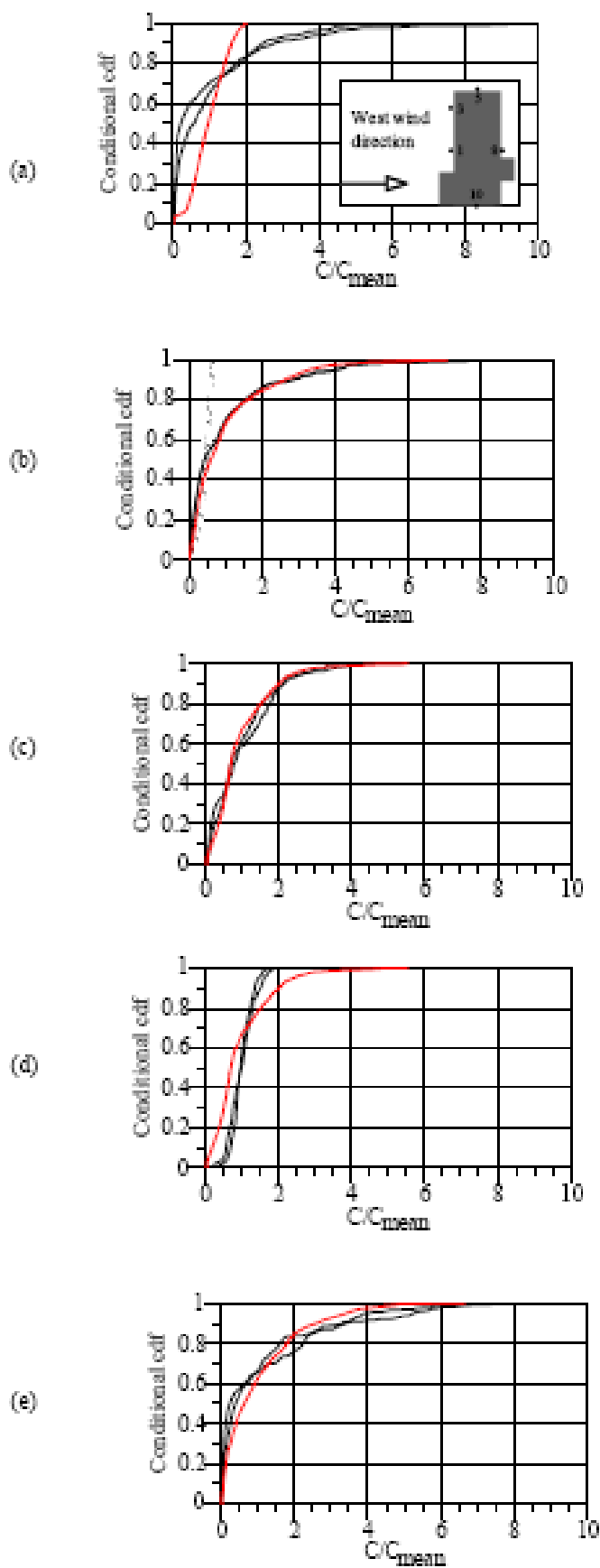


Figure 09 - Conditional cdf's in neutral conditions for source located upwind of the centre of the long face of the building. — Exp. 3 and - - - - Exp.4 Santos et al. (2005), — Simulation: (a) sensor 1, (b) sensor 3, (c) sensor 5, (d) sensor 8 and (e) sensor 10.

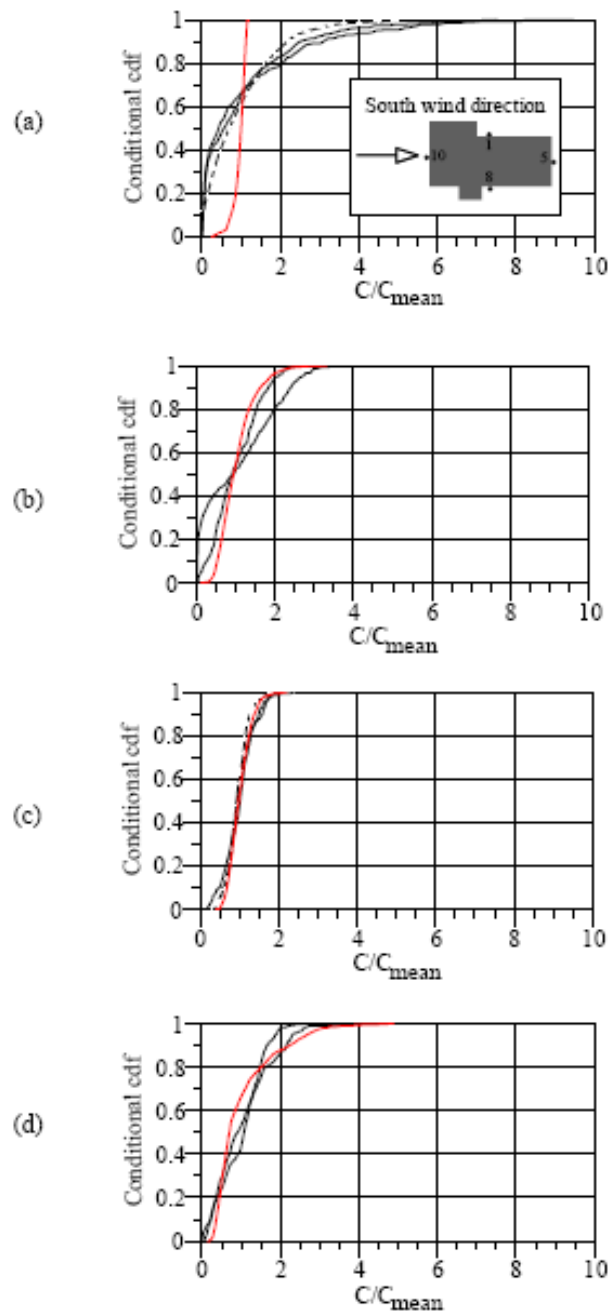


Figure 10 - Conditional cdf's in neutral conditions for source located upwind of the short face of the building. — Exp. 1 and - - - Exp. 2 Santos et al. (2005), — Simulation: (a) sensor 1, (b) sensor 3, (c) sensor 5, (d) sensor 8 and (e) sensor 10.

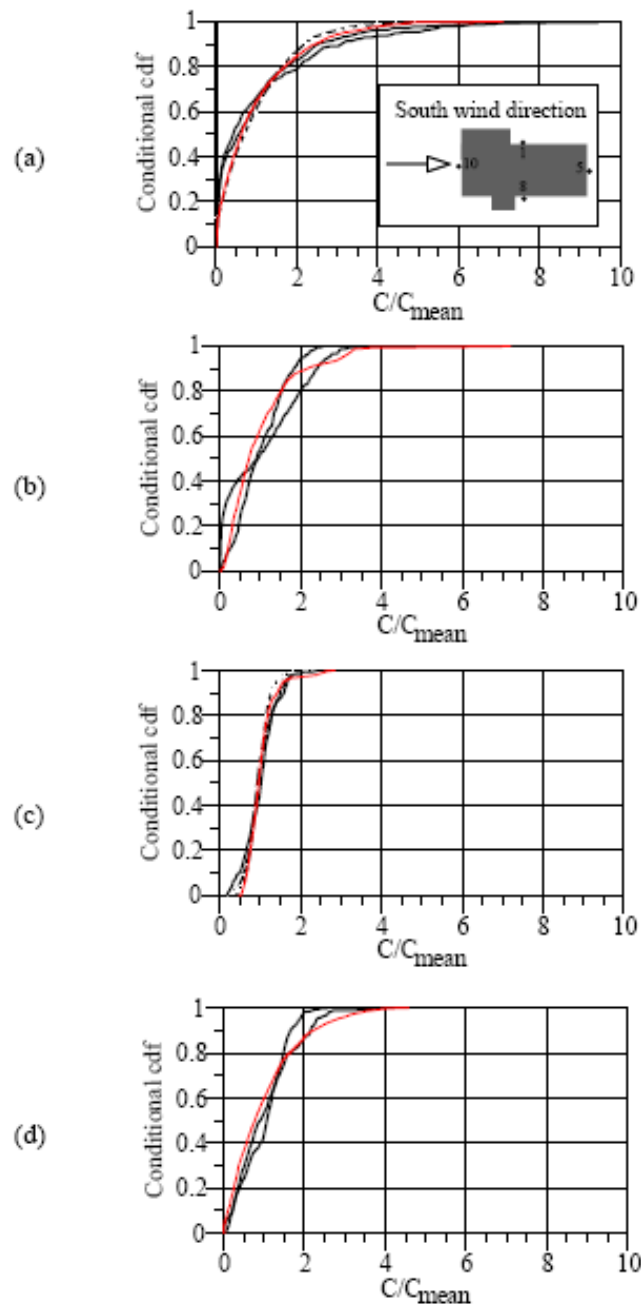


Figure 11 - Conditional cdf's in neutral conditions for source located upwind of the centre of the shorter face of the building, — Exp. 1 and - - - - Exp. 2 Santos et al. (2005), — Simulation with high-density roughness: (a) sensor 1, (b) sensor 3, (c) sensor 5, (d) sensor 8 and (e) sensor 10.

Figures 9, 10 and 11 present the function of cumulative frequency which represents the Cumulative Density Function (cdf) of concentration, for different sensors. The cdf gives the proportion of concentration readings which are below a given concentration (expressed as the ratio between the 1 sec averaged and mean concentration values).

Figure 9 shows the cdf for monitors 1, 3, 5, 8 and 10 for the simulation with the west wind direction impinging on the larger face of the building. In Figures 9b, 9c and 9e, the cdf presented satisfactory performance. The simulation results presented in Figures 9a and 9d did not correspond to the experimental data. In Figure 9a, the behaviour of the cdf indicates that there was a low fluctuation of the concentration since the slope of the fluctuation intensity curve obtained is high. As stated earlier, this low fluctuation of the concentration is caused by the velocity profile set at the inlet being an average profile. Thus, less flow turbulence structures are developed. The same episode is observed in Figure 10a.

In Figures 10b, 10c and 10d, the cdf's shape obtained by the simulation is satisfactory comparing to the experimental data.

In Figure 11, with the high-density roughness elements located close to the inlet, the turbulence intensity levels that reach the building are greater than the other simulations without the high-density roughness elements. This fact

provides a better representation of the concentration fluctuation intensity. The cdf's showed in Figure 11 are satisfactory, since the shape of the cdf's correspond to those obtained in field experiments.

5. CONCLUSIONS

Three different simulations using the LES turbulence model were performed in order to study the behaviour of the pollutant dispersion around a complex shaped building, the results obtained were compared with field experiments results obtained by Santos et al (2005). Two simulations involving smooth surface were achieved, one where the west wind direction impinged on the larger face of the building and the other where the south wind direction impinged the shorter face of the building. Both predicted low turbulence intensity levels which leads to less pollutant dispersion and generates a high pollutant concentration at the building location. These results can be explained by the velocity profile of the inlet which is an average and does not present any fluctuation.

The closest mean concentrations and concentration fluctuation intensity to the field experiments were observed with the third simulation. This latter used a high-density roughness elements placed close to the inlet with a west wind direction impinging on the larger face of the building. This method enables to obtain predictions of higher dispersion of pollutants nearby the building vicinity. Indeed, the roughness surface leads to a higher structure turbulence development which causes high levels of concentration fluctuation.

4. REFERENCES

- Cheng, Y., Lien, F.S., Yee, E., Sinclair, R., "A comparison of large eddy simulations with a standard k- ϵ Reynolds averaged Navier-Stokes models for the prediction of a fully developed turbulent flow over a matrix of cubes", *Journal of Wind Engineering and Industrial Aerodynamics*, Vol. 91, pp. 1301-1328, 2003
- Iaccarino, G.; Ooi, A.; Durbin, P.A.; Behnia, M., "Reynolds averaged simulation of unsteady separated flow. *International Journal of Heat and Fluid Flow*", Vol. 24, pp. 147-156, 2003.
- Jiang, Y.; Chen Q., "Study of natural ventilation in buildings by large eddy simulation", *Journal of Wind Engineering and Industrial Aerodynamics*, Vol. 89, pp. 1155-1178, 2001.
- Lim, H. C., Thomas, T. G., Castro, I. P., "Flow around a cube in a turbulent boundary layer: LES and experiment", *Journal of Wind Engineering and Industrial Aerodynamics*, vol. 97, Issue 2, pp 96 - 109.
- Lund, T. S.; Wu, X.; Squires K. D., "Generation of turbulent inflow data for spatially developing boundary simulation", *J. Comput. Phys*, Vol. 140, pp. 233-258, 1998.
- Mavroidis, I. "Atmospheric dispersion around buildings", 1997. 346 f. Ph.D. Thesis. Department of Chemical Engineering. University of Manchester. England, 1997.
- Murakami, S., "Future trends in computational wind engineering", *Journal of Wind Engineering and Industrial Aerodynamics*, Vol. 67 e 68, pp. 3-34, 1997.
- Murakami, S.; Mochida, A.; Ooka, R.; Kato, S.; Lizuka, S., "Numerical prediction of flow around a building with various turbulence models: comparison of κ - ϵ EVM, ASM, DSM and LES with Wind tunnel tests", *ASHRAE Transactions*, 1996.
- Murakami S. (1993), "Comparison of Various Turbulence Models Applied to a Bluff Body", *Journal of Wind Eng. and Ind. Aero.*, vol. 46,47, pp. 21-36.
- Nozawa, K.; Tamura, T., "Large Eddy Simulation of the flow around a low-rise building immersed in a rough-wall turbulent boundary layer", *Journal of Wind Engineering and Industrial Aerodynamics*, Vol. 90-12, pp. 1151-1162, 2002.
- Rodi, W., "Comparison of LES and RANS calculations of the flow around bluff bodies", *Journal of Wind Engineering and Industrial Aerodynamics*. Vol. 69-71, pp. 55-75, 1997.
- Sada, K.; Sato, A., "Numerical calculation of flow and stack-gas concentration fluctuation around a cubical building", *Atmospheric Environment*, Vol. 36, pp. 5527-5534, 2002.
- Santos, J. M.; Griffiths, R. F.; Roberts, I. D.; Reis, N. C., "A field experiment on turbulent concentration fluctuations of an atmospheric tracer gas in the vicinity of a complex-shaped building". *Atmospheric Environment*, Vol. 39, pp. 4999-5012, 2005.

Santos, J. M., “Flow and Dispersion Around Isolated Buildings” 2000. 257 f. Ph.D. Thesis. Department of Chemical Engineering. University of Manchester, United Kingdom, 2000.

Senthoran, S., Lee, D. D., Parameswaram, S., “A computational model to calculate the flow-induced pressure fluctuations on building. “Journal of Wind Engineering and Industrial Aerodynamics”, Vol. 92, pp.1131-1145, 2004.
Yakhot, A., Liu, H.; Nikitin, N.. “Turbulent flow around a wall-mounted cube: A direct numerical simulation”, International Journal of Heat and Fluid Flow, Vol. 27, pp. 994–1009, 2006.